

Joint resummation for pion wave function and pion transition form factor

Hsiang-nan Li^{a,b,c}, Yue-Long Shen^d, Yu-Ming Wang^{e,f} *

^a*Institute of Physics, Academia Sinica, Taipei, Taiwan 115, Republic of China*

^b*Department of Physics, National Cheng-Kung University, Tainan, Taiwan 701, Republic of China*

^c*Department of Physics, National Tsing-Hua University, Hsinchu, Taiwan 300, Republic of China*

^d*College of Information Science and Engineering, Ocean University of China, Qingdao, Shandong 266100, P.R. China*

^e*Institut für Theoretische Teilchenphysik und Kosmologie RWTH Aachen D - 52056 Aachen, Germany*

^f*Physik Department T31, James-Franck-Straße, Technische Universität München, D-85748 Garching, Germany*

ABSTRACT: We construct an evolution equation for the pion wave function in the k_T factorization theorem, whose solution sums the mixed logarithm $\ln x \ln k_T$ to all orders, with x (k_T) being a parton momentum fraction (transverse momentum). This joint resummation induces strong suppression of the pion wave function in the small x and large b regions, b being the impact parameter conjugate to k_T , and improves the applicability of perturbative QCD to hard exclusive processes. The above effect is similar to those from the conventional threshold resummation for the double logarithm $\ln^2 x$ and the conventional k_T resummation for $\ln^2 k_T$. Combining the evolution equation for the hard kernel, we are able to organize all large logarithms in the $\gamma^* \pi^0 \rightarrow \gamma$ scattering, and to establish a scheme-independent k_T factorization formula. It will be shown that the significance of next-to-leading-order contributions and saturation behaviors of this process at high energy differ from those under the conventional resummations. It implies that QCD logarithmic corrections to a process must be handled appropriately, before its data are used to extract a hadron wave function. Our predictions for the involved pion transition form factor, derived under the joint resummation with the input of non-asymptotic pion wave functions, match reasonably well the CLEO-c, BaBar, and Belle data.

KEYWORDS: Resummation, Factorization, Pion transition form factor.

*Aachen: TTK-13-22, SFB/CPP-13-75; Munich: TUM-HEP-902/13.

Contents

| | |
|------------------------------------------------------------------|-----------|
| 1. INTRODUCTION | 1 |
| 2. EVOLUTION EQUATION | 3 |
| 2.1 Evolution kernel | 4 |
| 2.2 Solution in Mellin and impact-parameter spaces | 7 |
| 3. RESUMMATION IMPROVED WAVE FUNCTIONS | 9 |
| 3.1 Resummation with fixed α_s | 11 |
| 3.2 Resummation with running α_s | 14 |
| 4. PION TRANSITION FORM FACTOR | 18 |
| 4.1 k_T factorization formula | 19 |
| 4.2 Numerical analysis | 20 |
| 5. CONCLUSION AND DISCUSSION | 22 |
| A. Explicit expressions of the functions F_i | 23 |

1. INTRODUCTION

Great efforts have been devoted to the extension of the k_T factorization theorem for exclusive processes [1, 2, 3, 4, 5, 6] to subleading levels recently. The next-to-leading-order (NLO) corrections to the pion transition (electromagnetic) form factor associated with the $\pi\gamma^* \rightarrow \gamma(\pi)$ scattering have been calculated at leading power [7, 8]. Those to the $B \rightarrow \pi$ transition form factors involved in B meson semileptonic decays were derived in [9]. Up to subleading power, the three-parton contributions to the pion electromagnetic form factor, to the $B \rightarrow \gamma$ transition form factor, and to the $B \rightarrow \pi$ transition form factors have been studied in [10], [11], and [12], respectively. A k_T -dependent hard kernel is defined as the difference between QCD diagrams and effective diagrams for transverse-momentum-dependent (TMD) hadron wave functions. Therefore, to obtain a NLO hard kernel, both QCD diagrams and effective diagrams need to be evaluated to the same level. The NLO analysis of the B meson and pion wave functions have revealed various important logarithms, which stimulate corresponding resummation formalisms for their organization to all orders in the coupling constant.

It has been known [13] that a TMD hadron wave function contains the light-cone singularity from the region with a loop momentum parallel to a Wilson line on the light cone. To regularize the light-cone singularity, one may rotate the Wilson line away from

the light cone to an arbitrary direction u with $u^2 \neq 0$ [13, 14]. The higher-order wave function then depends on u^2 through the scale $\zeta_P^2 \equiv 4(P \cdot u)^2/u^2$, where P denotes the hadron momentum. The variation of u , namely, of ζ_P^2 introduces a factorization-scheme dependence into the hadron wave function. The evaluation of the NLO effective diagrams for the B meson wave function indicates the existence of the logarithms $\ln^2(\zeta_P^2/m_B^2)$ and $\ln x \ln(\zeta_P^2/m_B^2)$ [9], m_B being the B meson mass and x being the momentum fraction of the spectator. The NLO diagrams for the pion wave function produce the mixed logarithm $\ln x \ln(\zeta_P^2/k_T^2)$ [8], k_T being the parton transverse momentum. All the above logarithms become large as $u^2 \rightarrow 0$, and as x and k_T are small, which is the dominant kinematic region in the k_T factorization theorem for exclusive processes. The logarithms in the B meson wave function have been organized under the rapidity resummation [15], whose effect was shown to diminish the B meson wave function at the end point $x = 0$.

The above observation hints that the resummation of the mixed logarithm $\ln x \ln(\zeta_P^2/k_T^2)$ for the pion wave function would modify both the x and k_T dependencies. It then calls for the joint resummation [16, 17, 18, 19], which was proposed to unify the conventional threshold resummation for $\ln^2 x$ [20, 21, 22] and the conventional k_T resummation for $\ln^2 k_T$ [14, 23]. For a recent review on this subject, see [24]. In this paper we will construct an evolution equation in the scale ζ_P^2 following the idea in [17], whose solution resums the mixed logarithm in the Mellin (N , conjugate to x) and impact-parameter (b , conjugate to k_T) spaces. The inverse Mellin transformation is then applied to get the x dependence of the pion wave function. It will be demonstrated that the joint resummation induces suppression which is stronger at small x than at moderate x , and intensifies with increase of b . This effect, similar to those of the threshold and k_T resummations, improves the applicability of perturbative QCD (PQCD) to hard exclusive processes. Combining the evolution equation for the hard kernel of the $\gamma^* \pi^0 \rightarrow \gamma$ scattering, we organize all the relevant large logarithms, and remove the factorization-scheme dependence on ζ_P^2 mentioned before. This is the first time that the k_T factorization for a simple exclusive process can be made scheme independent in the presence of the light-cone singularity.

It has been known that $\gamma^* \pi^0 \rightarrow \gamma$ serves as an ideal process for the determination of the pion wave function, and the involved pion transition form factor $F(Q^2)$, Q^2 being the momentum transfer squared, has been studied thoroughly. In particular, it was claimed that the quantity $Q^2 F(Q^2)$ begins to saturate at relatively low Q^2 as calculated in QCD sum rules (QCDSR) [25]. We will analyze the leading-order (LO) and NLO contributions to the pion transition form factor with inputs of different model wave functions, including the asymptotic model, the flat model, and the model with the second Gegenbauer moment. The results are compared to those from the PQCD approach [26], that incorporates the conventional threshold and k_T resummations. It will be observed that the significance of the NLO correction to and the saturation behavior of $Q^2 F(Q^2)$ differ under the joint resummation and the conventional resummations. It implies that QCD logarithmic corrections to a process must be handled appropriately, before its data are used to extract a hadron wave function. Our predictions for $Q^2 F(Q^2)$ with the input of non-asymptotic pion wave functions match reasonably well the CLEO-c, BaBar, and Belle data, which seem to indicate scaling violation at currently accessible Q^2 .

In Sec. 2 we construct the evolution equation for the resummation of the mixed logarithm in the pion wave function, and then solve it in the Mellin and impact-parameter spaces. The inverse Mellin transformation of the solution is performed in Sec. 3, with different initial conditions of the evolution. Note that the running of the strong coupling constant down to the low energy region has to be modified in order to avoid the Landau pole. The joint resummation effect on the x and b dependencies of the pion wave function is then investigated. In Sec. 4 the pion transition form factor is evaluated for a given model wave function at the LO and NLO levels under the joint resummation and the conventional resummations. The different results for the NLO contributions and for the saturation behaviors at high energy are compared. We summarize our findings, and discuss potential extension of our formalism to more complicated processes in Sec. 5. The explicit expressions for the solutions of the evolution equation are collected in Appendix A.

2. EVOLUTION EQUATION

The TMD pion wave function $\Phi(x, k_T)$ is defined by the non-local hadron-to-vacuum matrix element ¹

$$\Phi(x, k_T, \zeta^2, \mu_f) = \int \frac{dy^+}{2\pi} \frac{d^2 y_T}{(2\pi)^2} e^{-ixP^- y^+ + i\mathbf{k}_T \cdot \mathbf{y}_T} \times \langle 0 | \bar{q}(y) W_y(u)^\dagger I_{u;y,0} W_0(u) \not{n}_+ \gamma_5 q(0) | \pi(P) \rangle, \quad (2.1)$$

where μ_f is the factorization scale, the coordinate $y = (y^+, 0, \mathbf{y}_T)$ is off the light cone generally, and xP^- and \mathbf{k}_T are the longitudinal and transverse momenta carried by the anti-quark \bar{q} , respectively. A TMD hadron wave function describes the distributions of a light parton in both light-ray and transverse directions. To maintain the gauge invariance of the definition in Eq. (2.1), the gauge-link operator $W_y(u)$

$$W_y(u) = \mathcal{P} \exp \left[-ig \int_0^\infty d\lambda u \cdot A(y + \lambda u) \right], \quad (2.2)$$

has been introduced, where g is the QCD coupling constant, and \mathcal{P} denotes the path-ordered exponential. The non-light-like vector u differs from the usual Wilson line direction $n_+ = (1, 0, \mathbf{0}_T)$, and plays a role of the regulator for the light-cone divergences [13]. The transverse gauge link $I_{u;y,0}$, unraveling the cusp obstruction in the contour of the Wilson lines at infinity, does not contribute in the covariant gauge [28].

As extracting a NLO hard kernel in the k_T factorization formula of a pion-induced process, the infrared subtraction defined as the convolution of the NLO pion wave function with the LO hard kernel is performed. The QCD correction to the pion wave function gives rise to the mixed logarithm $\ln x \ln(\zeta^2 P^{-2}/k_T^2)$ [7, 8, 9], with the dimensionless rapidity parameter

$$\zeta^2 = \frac{4(n_- \cdot u)^2}{u^2}, \quad (2.3)$$

¹The leading-twist light-cone projector for a pion in the collinear factorization can be found in [27].

$n_- = (0, 1, \mathbf{0}_T)$ being a light-like vector along the pion momentum P . The double rapidity logarithm $\ln^2 \zeta^2$ in the B meson case is absent here because of the color-transparency mechanism for an energetic pion, which suppresses soft gluon contributions.

The goal of this section is to construct an evolution equation, whose solution sums the mixed logarithm in the pion wave function. Following [17], we trade the derivative with respect to the rapidity parameter ζ^2 for the variation of the Wilson link direction u ,

$$\zeta^2 \frac{d}{d\zeta^2} \Phi = - \frac{u^2}{n_- \cdot u} \frac{n_-^\alpha}{2} \frac{d}{du^\alpha} \Phi. \quad (2.4)$$

It is obvious that this chain rule simplifies the analysis dramatically as the u dependence appears only through the Wilson line interactions. Applying Eq. (2.4) to the Feynman rule associated with the Wilson link, we have

$$\zeta^2 \frac{d}{d\zeta^2} \frac{u^\beta}{u \cdot l + i\epsilon} = \frac{\hat{u}^\beta}{2u \cdot l}, \quad (2.5)$$

with the special vertex

$$\hat{u}^\beta = \frac{u^2}{n_- \cdot u} \left(\frac{n_- \cdot l}{u \cdot l} u^\beta - n_-^\beta \right). \quad (2.6)$$

We will derive the rapidity evolution equation

$$\zeta^2 \frac{d}{d\zeta^2} \Phi(x, k_T, \zeta^2, \mu_f) = \Gamma(x, k_T, \zeta^2) \otimes \Phi(x, k_T, \zeta^2, \mu_f), \quad (2.7)$$

where \otimes represents convolutions in the momentum fraction x and the transverse momentum k_T , and the evolution kernel Γ involves the diagrams with the special vertex.

2.1 Evolution kernel

It is easy to see that the structure of the special vertex suppresses a collinear gluon contribution to Γ [15]. The evolution kernel is then dominated by soft and hard gluon exchanges, usually denoted as the functions K and G , respectively. The soft and hard gluon radiations off the active quark, as shown in Fig. 1, lead to

$$K_1 = - \frac{ig^2 C_F}{2} \int \frac{d^4 l}{(2\pi)^4} \frac{\hat{u} \cdot n_-}{(u \cdot l + i\epsilon)(l^2 + i\epsilon)(n_- \cdot l + i\epsilon)}, \quad (2.8)$$

$$K_2 \otimes \Phi = \frac{ig^2 C_F}{2} \int \frac{d^4 l}{(2\pi)^4} \frac{\hat{u} \cdot n_-}{(u \cdot l + i\epsilon)(l^2 + i\epsilon)(n_- \cdot l + i\epsilon)} \\ \times \Phi(x - l^-/P^-, |\mathbf{k}_T - \mathbf{l}_T|, \zeta^2, \mu_f), \quad (2.9)$$

for the function K , and

$$G_1 = - \frac{ig^2 C_F}{2} \int \frac{d^4 l}{(2\pi)^4} \frac{(\bar{x} P + l) \not{l}}{(u \cdot l + i\epsilon)(l^2 + i\epsilon)[(\bar{x} P + l)^2 + i\epsilon]}, \\ G_2 = K_1, \quad (2.10)$$

for the function G with the variable $\bar{x} \equiv 1 - x$.

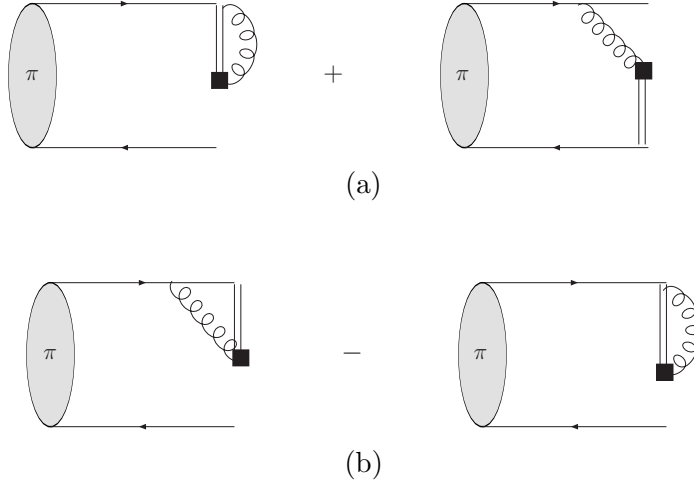


Figure 1: (a) diagrams for the function K from soft gluon exchanges between the Wilson lines and the active quark, and (b) diagrams for the function G from hard gluon exchanges, where the box denotes the special vertex. The second diagram in the function G is included to avoid the double counting of the soft contribution. Those diagrams with gluon radiations off the spectator quark are not shown here.

Adopting the dimensional regularization for the ultraviolet divergence and introducing the gluon mass λ for the infrared divergence, we obtain

$$K_1 = -\frac{\alpha_s C_F}{4\pi} \left(\frac{1}{\epsilon} - \gamma_E + \ln \frac{4\pi\mu^2}{\lambda^2} \right). \quad (2.11)$$

Because the soft divergences cancel between K_1 and K_2 , and between G_1 and G_2 , the gluon mass λ will approach to zero eventually. For the evaluation of K_2 , we apply the Mellin and Fourier transformations

$$\tilde{\Phi}(N, b, \zeta^2, \mu_f) = \int_0^1 dx (1-x)^{N-1} \int \frac{d^2 k_T}{(2\pi)^2} \exp(i\mathbf{k}_T \cdot \mathbf{b}) \Phi(x, k_T, \zeta^2, \mu_f), \quad (2.12)$$

b being the impact parameter. Equation (2.9) then gives $\tilde{K}_2 \tilde{\Phi}(N, b, \zeta^2, \mu_f)$ with the soft kernel

$$\begin{aligned} \tilde{K}_2 &= \frac{ig^2 C_F}{2} \int \frac{d^4 l}{(2\pi)^4} \left(1 - \frac{l^-}{P^-} \right)^{N-1} \exp(-il_T \cdot \mathbf{b}) \frac{\hat{u} \cdot n_-}{(u \cdot l + i\epsilon)(l^2 + i\epsilon)(n_- \cdot l + i\epsilon)}, \\ &= \frac{\alpha_s C_F}{2\pi} \left[K_0(\lambda b) - K_0\left(\frac{\zeta P^- b}{N}\right) \right], \end{aligned} \quad (2.13)$$

in which the terms suppressed by powers of $1/\zeta^2$ have been dropped, and K_0 is the zeroth-order modified Bessel function of the second kind. Hence, the function K is written as

$$\tilde{K}^{(b)} = K_1 + \tilde{K}_2 = -\frac{\alpha_s C_F}{4\pi} \left(\frac{1}{\epsilon} - \gamma_E + \ln \frac{4\pi\mu^2 N^2}{\zeta^2 P^{-2}} \right), \quad (2.14)$$

where the large- N expansion of Eq. (2.13) has been made, and the superscript (b) labels the bare function explicitly.

The hard function G can be calculated following the same line, and reads

$$G^{(b)} = G_1 - G_2 = \frac{\alpha_s C_F}{4\pi} \left[\frac{1}{\epsilon} - \gamma_E + \ln \frac{4\pi\mu^2}{\zeta^2(\bar{x}P^-)^2} - 4 \right]. \quad (2.15)$$

We will adopt the approximation $\bar{x} \approx 1$ in the small x region, where the mixed logarithm plays a significant role. It is found that both the soft and hard functions depend on the factorization scale μ , and such a dependence cancels in their sum. This fact is attributed to the μ independence of the mixed logarithm that we are going to resum.

Applying the modified minimal subtraction ($\overline{\text{MS}}$) scheme to the ultraviolet renormalization yields

$$\begin{aligned} \tilde{K}^{(r)}(\mu) &= -\frac{\alpha_s C_F}{2\pi} \ln \frac{\mu N}{\zeta P^-}, & \lambda_{\tilde{K}} &= \mu \frac{d\tilde{K}}{d\mu} = \frac{\alpha_s C_F}{2\pi}, \\ G^{(r)}(\mu) &= \frac{\alpha_s C_F}{2\pi} \left(\ln \frac{\mu}{\zeta P^-} - 2 \right), & \lambda_G &= \mu \frac{dG}{d\mu} = -\lambda_{\tilde{K}}, \end{aligned} \quad (2.16)$$

where the additive counterterms δK (δG) of the function $\tilde{K}^{(b)}$ ($G^{(b)}$) can be read from Eq. (2.14) (Eq. (2.15)). The renormalization-group (RG) equations for the soft and hard functions are then given, in terms of the anomalous dimensions $\lambda_{\tilde{K}}$ and λ_G , by

$$\mu \frac{d\tilde{K}^{(r)}}{d\mu} = -\lambda_{\tilde{K}}, \quad \mu \frac{dG^{(r)}}{d\mu} = -\lambda_G, \quad (2.17)$$

which lead to the RG improved evolution kernel

$$\tilde{K}^{(r)}(\mu) + G^{(r)}(\mu) = \tilde{K}^{(r)}(\mu_0) + G^{(r)}(\mu_1) - \int_{\mu_0}^{\mu_1} \frac{d\tilde{\mu}}{\tilde{\mu}} \lambda_K(\tilde{\mu}). \quad (2.18)$$

We choose the scales

$$\mu_0 := \mu_0(\zeta) = \frac{\zeta P^-}{N}, \quad \mu_1 := \mu_1(\zeta) = e^2 \zeta P^-, \quad (2.19)$$

to diminish the initial conditions $\tilde{K}^{(r)}(\mu_0)$ and $G^{(r)}(\mu_1)$.

The evolution kernel Γ also contains the diagrams with gluon radiations from the spectator quark in principle. However, these diagrams contribute at the next-to-leading logarithmic level, because the NLO effective diagrams with gluon radiations off the spectator quark do not generate the mixed logarithm $\ln x \ln(\zeta^2 P^{-2}/k_T^2)$ as indicated by Eqs. (36) and (37) in [9]. The corresponding soft and hard functions are expressed as

$$\begin{aligned} K'_1 &= G'_2 = K_1, \\ K'_2 \otimes \Phi &= K_2 \otimes \Phi, \\ G'_1 &= \frac{ig^2 C_F}{2} \int \frac{d^4 l}{(2\pi)^4} \frac{(x P^- - l) \not{l}}{(u \cdot l + i\epsilon)(l^2 + i\epsilon)[(xP - l)^2 + i\epsilon]}, \end{aligned} \quad (2.20)$$

which yield

$$G'^{(b)} = G'_1 - G'_2 = \frac{\alpha_s C_F}{4\pi} \left[\frac{1}{\epsilon} - \gamma_E + \ln \frac{4\pi\mu^2}{\zeta^2(xP^-)^2} - 4 \right]. \quad (2.21)$$

The logarithm $\ln x$ in the soft function $K'_2 \otimes \Phi$ can be extracted by implementing the approximation [16]

$$\Phi(x - l^-/P^-, |\mathbf{k}_T - \mathbf{l}_T|, \zeta^2, \mu_f) \approx \theta(xP^- - l^-) \Phi(x, k_T, \zeta^2, \mu_f), \quad (2.22)$$

under which we obtain

$$\begin{aligned} K'_2 &= \frac{ig^2 C_F}{2} \int \frac{d^4 l}{(2\pi)^4} \frac{\hat{u} \cdot n}{(u \cdot l + i\epsilon)(l^2 + i\epsilon)(n_- \cdot l + i\epsilon)} \theta(xP^- - l^-), \\ &= \frac{\alpha_s C_F}{2\pi} \ln \frac{\zeta x P^-}{\lambda}. \end{aligned} \quad (2.23)$$

The cancelation of the soft divergences between $K'_1 (= K_1)$ in Eq. (2.11) and K'_2 in Eq. (2.23) is evident, whose sum gives

$$K'^{(b)} = K'_1 + K'_2 = -\frac{\alpha_s C_F}{4\pi} \left[\frac{1}{\epsilon} - \gamma_E + \ln \frac{4\pi\mu^2}{\zeta^2 (xP^-)^2} \right]. \quad (2.24)$$

Applying the $\overline{\text{MS}}$ scheme to the bare soft and hard functions gives the renormalized ones

$$K'^{(r)} = -\frac{\alpha_s C_F}{2\pi} \ln \frac{\mu}{x \zeta P^-}, \quad (2.25)$$

$$G'^{(r)} = \frac{\alpha_s C_F}{2\pi} \left(\ln \frac{\mu}{x \zeta P^-} - 2 \right). \quad (2.26)$$

Obviously, the logarithms of the renormalization scale and the momentum fraction cancel in the sum $K'^{(r)} + G'^{(r)}$, implying that a RG treatment is not necessary here, and that it produces only a next-to-leading logarithm as stated above. Hence, this contribution can be absorbed into the solution of the evolution equation by tuning the initial rapidity parameter ζ , whose variation within the order-unity range causes a next-to-leading logarithmic effect. We will take advantage of the freedom in choosing the bounds of ζ to achieve the matching between the resummation formula and the NLO results of the pion transition form factor. That is, the summation of the above next-to-leading logarithms can be taken care of by the matching procedure, and the kernel $K'^{(r)} + G'^{(r)}$ will be neglected below.

2.2 Solution in Mellin and impact-parameter spaces

Equation (2.7) under the Mellin and Fourier transformations becomes

$$\zeta^2 \frac{d}{d\zeta^2} \tilde{\Phi}(N, b, \zeta^2, \mu_f) = \tilde{\Gamma}(N, b, \zeta^2) \tilde{\Phi}(N, b, \zeta^2, \mu_f), \quad (2.27)$$

with the evolution kernel

$$\tilde{\Gamma}(N, b, \zeta^2) = \tilde{K}^{(r)}(\mu) + G^{(r)}(\mu) = - \int_{\mu_0(\zeta)}^{\mu_1(\zeta)} \frac{d\tilde{\mu}}{\tilde{\mu}} \lambda_K(\tilde{\mu}). \quad (2.28)$$

Solving the differential equation (2.27), we get

$$\begin{aligned} \tilde{\Phi}(N, b, \zeta^2, \mu_f) &= \exp \left\{ - \int_{\zeta_0^2}^{\zeta^2} \frac{d\tilde{\zeta}^2}{\tilde{\zeta}^2} \left[\int_{\mu_0(\tilde{\zeta})}^{\mu_1(\tilde{\zeta})} \frac{d\tilde{\mu}}{\tilde{\mu}} \lambda_K(\tilde{\mu}) \theta(\mu_1(\tilde{\zeta}) - \mu_0(\tilde{\zeta})) \right] \right\} \\ &\times \tilde{\Phi}(N, b, \zeta_0^2, \mu_f), \end{aligned} \quad (2.29)$$

which constitutes one of the main technical results of this paper. The initial rapidity parameter ζ_0 will be specified later, and the step function in the exponent will become effective as we perform the inverse Mellin transformation.

Apart from the mixed logarithm, the NLO pion wave function contains the single logarithm $\ln(\mu_f/Q)$, which can be summed via the standard RG equation

$$\mu_f \frac{d}{d\mu_f} \tilde{\Phi}(N, b, \zeta^2, \mu_f) = -\gamma_\pi(\mu_f) \tilde{\Phi}(N, b, \zeta^2, \mu_f), \quad (2.30)$$

with the anomalous dimension [8]

$$\gamma_\pi(\mu_f) = -\frac{3}{2} \frac{\alpha_s(\mu_f) C_F}{\pi}. \quad (2.31)$$

Combining the joint resummation and the solution to Eq. (2.30) leads to

$$\begin{aligned} \tilde{\Phi}(N, b, \zeta^2, \mu_f) = \exp \left\{ - \int_{\zeta_0^2}^{\zeta^2} \frac{d\tilde{\zeta}^2}{\tilde{\zeta}^2} \left[\int_{\mu_0(\tilde{\zeta})}^{\mu_1(\tilde{\zeta})} \frac{d\tilde{\mu}}{\tilde{\mu}} \lambda_K(\tilde{\mu}) \theta(\mu_1(\tilde{\zeta}) - \mu_0(\tilde{\zeta})) \right] \right. \\ \left. + \frac{3}{2} \int_{\mu_i}^{\mu_f} \frac{d\tilde{\mu}}{\tilde{\mu}} \frac{\alpha_s(\tilde{\mu}) C_F}{\pi} \right\} \tilde{\Phi}(N, b, \zeta_0^2, \mu_i), \end{aligned} \quad (2.32)$$

where μ_i is the initial scale of the RG evolution.

Note that the physical form factor

$$F(Q^2) = \tilde{\Phi}(N, b, \zeta^2, \mu_f) \otimes \tilde{H}(N, b, \zeta^2, Q^2, \mu_f), \quad (2.33)$$

is independent of the factorization scheme and the factorization scale μ_f , where \tilde{H} denotes the hard kernel in the Mellin and impact-parameter spaces. Therefore, we have the evolution equation

$$\zeta^2 \frac{d}{d\zeta^2} \tilde{H}(N, b, \zeta^2, Q^2, \mu_f) = -\tilde{\Gamma}(N, b, \zeta^2) \tilde{H}(N, b, \zeta^2, Q^2, \mu_f), \quad (2.34)$$

for the joint resummation, and the RG equation

$$\mu_f \frac{d}{d\mu_f} \tilde{H}(N, b, \zeta^2, Q^2, \mu_f) = \gamma_\pi(\mu_f) \tilde{H}(N, b, \zeta^2, Q^2, \mu_f). \quad (2.35)$$

The solution of the above two differential equations gives the resummation improved hard kernel

$$\begin{aligned} \tilde{H}(N, b, \zeta^2, Q^2, \mu_f) = \exp \left\{ \int_{\zeta^2}^{\zeta_1^2} \frac{d\tilde{\zeta}^2}{\tilde{\zeta}^2} \left[\int_{\mu_0(\tilde{\zeta})}^{\mu_1(\tilde{\zeta})} \frac{d\tilde{\mu}}{\tilde{\mu}} \lambda_K(\tilde{\mu}) \theta(\mu_1(\tilde{\zeta}) - \mu_0(\tilde{\zeta})) \right] \right. \\ \left. - \frac{3}{2} \int_t^{\mu_f} \frac{d\tilde{\mu}}{\tilde{\mu}} \frac{\alpha_s(\tilde{\mu}) C_F}{\pi} \right\} \tilde{H}(N, b, \zeta_1^2, Q^2, t), \end{aligned} \quad (2.36)$$

with the final rapidity parameter ζ_1 and the characteristic hard scale t . We make use of the freedom of choosing the bounds ζ_0^2 and ζ_1^2 for the joint resummation, such that the NLO

logarithmic enhancements in $\tilde{\Phi}(N, b, \zeta_0^2, \mu_i)$ and $\tilde{H}(N, b, \zeta_1^2, Q^2, t)$, displayed in Eqs. (39) and (40) of [7], respectively, are eliminated. This requires

$$\zeta_0^2 = \left(\frac{a N^{1/4}}{P^- b} \right)^2, \quad \zeta_1^2 = \tilde{a} N^{1/2}. \quad (2.37)$$

with the constants

$$a = \frac{e^{-1/4}}{2}, \quad \tilde{a} = (2e)^{-1/2}. \quad (2.38)$$

Inserting Eqs. (2.32) and (2.36) into Eq. (2.33), we derive

$$\begin{aligned} F(Q^2) &= \exp \left\{ - \int_{\zeta_0^2}^{\zeta_1^2} \frac{d\tilde{\zeta}^2}{\tilde{\zeta}^2} \left[\int_{\mu_0(\tilde{\zeta})}^{\mu_1(\tilde{\zeta})} \frac{d\tilde{\mu}}{\tilde{\mu}} \lambda_K(\tilde{\mu}) \theta(\mu_1(\tilde{\zeta}) - \mu_0(\tilde{\zeta})) \right] \right. \\ &\quad \left. + \frac{3}{2} \int_{\mu_i}^t \frac{d\tilde{\mu}}{\tilde{\mu}} \frac{\alpha_s(\tilde{\mu}) C_F}{\pi} \right\} \tilde{\Phi}(N, b, \zeta_0^2, \mu_i) \otimes \tilde{H}(N, b, \zeta_1^2, Q^2, t), \\ &\equiv \tilde{\Phi}(N, b, \zeta_1^2, t) \otimes \tilde{H}(N, b, \zeta_1^2, Q^2, t), \end{aligned} \quad (2.39)$$

which recapitulates the joint-resummation improved k_T factorization formula. The exponential factor in Eq. (2.39) describes the evolution from the initial condition $\tilde{\Phi}(N, b, \zeta_0^2, \mu_i)$ to the resummation improved wave function $\tilde{\Phi}(N, b, \zeta_1^2, t)$. We have confirmed that the expansion of the exponential factor up to $O(\alpha_s)$ reproduces the mixed logarithm and the single logarithm $\ln(1/N)$ in the NLO pion transition form factor [7]. Note that our resummation formalism was established in the conjugate space, while the calculation in [7] was performed in the momentum space. Hence, the correspondence between $\ln(1/N)$ in the former and $\ln x$ in the latter is not precise, and the matching condition confirmed above in fact suffers order-unity uncertainty at the next-to-leading-logarithmic level.

At last, we point out that the double logarithm $\ln^2(Q^2/k_T^2)$ in the TMD wave function and $\ln^2 x$ in the hard kernel were resummed in the conventional PQCD approach [7, 29]. Besides, the rapidity parameter ζ^2 was fixed to a specific value for convenience. Compared to the joint resummation, the double logarithm $\ln^2 \zeta$ in the TMD wave function has been ignored (see Eq. (37) in [7] for its existence), and the PQCD approach is not factorization-scheme independent, strictly speaking. That is, the formalism presented in this work represents a complete treatment of the logarithmic enhancement in the pion transition form factor, and the first scheme-independent k_T factorization formula.

3. RESUMMATION IMPROVED WAVE FUNCTIONS

In this section we explore the detailed properties of the resummation improved wave function $\tilde{\Phi}(N, b, \zeta_1^2, t)$. The factorization theorem for hard exclusive processes is usually formulated in the momentum-fraction space (see, however [30]). The inverse Mellin transformation for $\tilde{\Phi}(N, b, \zeta_1^2, t)$ gives

$$\overline{\Phi}(x, b, \zeta_1^2, t) = \int_{c-i\infty}^{c+i\infty} \frac{dN}{2\pi i} (1-x)^{-N} \tilde{\Phi}(N, b, \zeta_1^2, t), \quad (3.1)$$

where the parameter c is an arbitrary real number larger than the real part of the rightmost singularity of $\tilde{\Phi}(N, b, \zeta_1^2, t)$ in the complex N plane, and the Cauchy theorem can be applied to deform the integration contour whenever necessary. We will not implement the inverse Fourier transformation, so that the joint-resummation effect can be compared with the Sudakov-resummation effect directly, which is usually studied in the impact-parameter space.

The parametrization of the TMD pion wave function has been extensively discussed in the literature (for a recent discussion, see [31]). For simplicity, factorization of the initial pion wave function in the longitudinal and transverse momentum spaces

$$\Phi(x, k_T, \zeta_0^2, \mu_i) = \phi(x, \zeta_0^2, \mu_i) \Sigma(k_T^2), \quad (3.2)$$

will be postulated, albeit with the manifest violation of rotational invariance. Keep in mind that the major task of this section is to illustrate the joint-resummation effect. For definiteness, the transverse momentum distribution is taken as

$$\Sigma(k_T^2) = 4\pi\beta^2 \exp(-\beta^2 k_T^2), \quad (3.3)$$

where the prefactor is introduced to obey the normalization

$$\int \frac{d^2 k_T}{(2\pi)^2} \Sigma(k_T^2) = 1, \quad (3.4)$$

and the shape parameter β is related to the root mean square of the transverse momentum via

$$\langle \mathbf{k}_T^2 \rangle = \frac{\int_0^1 dx \int d^2 \mathbf{k}_T \mathbf{k}_T^2 |\Phi(x, k_T, \zeta_0^2, \mu_i)|^2}{\int_0^1 dx \int d^2 \mathbf{k}_T |\Phi(x, k_T, \zeta_0^2, \mu_i)|^2} = \frac{1}{2\beta^2}. \quad (3.5)$$

According to [32, 33], the input $\langle \mathbf{k}_T^2 \rangle^{1/2} = 350 \text{ MeV}$ that fulfills various constraints (including the $\pi \rightarrow \gamma\gamma$ decay rate) leads to $\beta = 2.0 \text{ GeV}^{-1}$.

The longitudinal momentum distribution $\phi(x, \zeta_0^2, \mu_i)$ is assumed to be the same as light-cone distribution amplitude (LCDA) $\varphi(x, \mu_i)$. The one-loop evolution equation indicates that the pion LCDA can be expanded in terms of the Gegenbauer polynomials $C_n^{3/2}$,

$$\varphi(x, \mu_i) = 6x(1-x) \sum_{n=0}^{\infty} a_n(\mu_i) C_n^{3/2}(2x-1), \quad (3.6)$$

where the odd Gegenbauer moments a_{2n+1} vanish due to symmetry prosperities. The dependence of a_{2n} on the scale μ_i is governed by the well-known Efremov-Radyushkin-Brodsky-Lepage equation [34, 35]. Along this line, we consider the following three models for the longitudinal momentum distribution

$$\begin{aligned} \phi^{\text{I}}(x, \zeta_0^2, \mu_i) &= 6x(1-x), \\ \phi^{\text{II}}(x, \zeta_0^2, \mu_i) &= 1, \\ \phi^{\text{III}}(x, \zeta_0^2, \mu_i) &= 6x(1-x) \left[1 + a_2 C_2^{3/2}(2x-1) \right], \end{aligned} \quad (3.7)$$

with the Gegenbauer polynomial $C_2^{3/2}(x) = (3/2)(5x^2 - 1)$.

The first model ϕ^I corresponds to the pion LCDA in the asymptotic limit. The flat distribution ϕ^{II} was proposed in [36, 37], where a nonperturbative correction beyond the operator product expansion was also introduced to explain the scaling violation indicated by the BaBar data. As there is overwhelming evidence that the pion LCDA at energy scales accessible in current experiments is broader than the asymptotic model, we keep the sub-leading Gegenbauer term in ϕ^{III} . The contribution from a higher Gegenbauer term to the pion transition form factor depends on the momentum transfer squared Q^2 and the shape parameter β [38]. Fitting to the Babar data, it has been observed that one can at best determine the second Gegenbauer moment and the shape parameter simultaneously in the framework of the k_T factorization [31]. For this reason, also expecting the quick convergence of the conformal spin expansion of the pion wave function (see, however, [39]), we will confine the analysis to the second Gegenbauer moment. Our formalism can be extended to include higher Gegenbauer terms straightforwardly.

3.1 Resummation with fixed α_s

To make our discussion more transparent, we start from the inverse Mellin transformation with a frozen coupling constant, and then generalize it to the case with a running coupling constant. With a frozen coupling α_s , the joint-resummation improved wave function $\tilde{\Phi}(N, b, \zeta_1^2, t)$ is easily deduced from Eq. (2.32)

$$\begin{aligned} \tilde{\Phi}(N, b, \zeta_1^2, t) = & \exp \left\{ \frac{\alpha_s C_F}{\pi} \left[-\ln \left(\frac{\tilde{a}}{a} P^- b \right) (\ln N + 2) + \frac{3}{2} \ln \left(\frac{t}{\mu_i} \right) \right] \right\} \\ & \times \tilde{\Phi}(N, b, \zeta_0^2, \mu_i). \end{aligned} \quad (3.8)$$

The exponential contains a branch cut on the negative real N axis and a singularity at $N = 0$. The analytical property of the wave function $\tilde{\Phi}(N, b, \zeta_1^2, t)$ also depends on the initial condition $\tilde{\Phi}(N, b, \zeta_0^2, \mu_i)$.

The Mellin and Fourier transformations defined in Eq. (2.12) lead the three models to

$$\tilde{\Phi}^I(N, b, \zeta_0^2, \mu_i) = \frac{6}{(N+1)(N+2)} \exp \left(-\frac{b^2}{4\beta^2} \right), \quad (3.9)$$

$$\tilde{\Phi}^{II}(N, b, \zeta_0^2, \mu_i) = \frac{1}{N} \exp \left(-\frac{b^2}{4\beta^2} \right), \quad (3.10)$$

$$\tilde{\Phi}^{III}(N, b, \zeta_0^2, \mu_i) = \frac{6}{(N+1)(N+2)} \left[1 + 6a_2 \frac{(N-1)(N-2)}{(N+3)(N+4)} \right] \exp \left(-\frac{b^2}{4\beta^2} \right). \quad (3.11)$$

As inserting the asymptotic model $\tilde{\Phi}^I(N, b, \zeta_0^2, \mu_i)$ into Eq. (3.8), $\tilde{\Phi}(N, b, \zeta_1^2, t)$ develops two additional poles at $N = -1$ and -2 . According to the Cauchy theorem, the contour for the inverse Mellin transformation is deformed as displayed in Fig. 2, which (i) runs from minus infinity towards $N = -2$ below the branching cut, (ii) slides into an infinitesimal semicircle around $N = -2$, (iii) continues toward $N = -1$ below the branching cut, (iv) slides into another infinitesimal semicircle around $N = -1$, (v) runs to $N = -r$ with $0 < r < 1$, (vi) revolves around the origin along a finite circle of radius r , and (vii) runs back to minus infinity in a way that reverses the steps (i)-(v) above the branching cut.

It is trivial to derive the joint-resummation improved pion wave function

$$\begin{aligned}
& \bar{\Phi}^I(x, b, \zeta_1^2, t) \\
&= 6 \exp\left(-\frac{b^2}{4\beta^2}\right) \exp\left\{\frac{\alpha_s C_F}{\pi} \left[-2\hat{a} + \frac{3}{2} \ln\left(\frac{t}{\mu_i}\right)\right]\right\} \\
&\times \left\{ \sum_{n=1}^2 (-1)^{n-1} (1-x)^n \exp[-\alpha_s C_F \hat{a} \ln n] \cos[\alpha_s C_F \hat{a}] \right. \\
&\quad + \int_{-\pi}^{\pi} \frac{d\varphi}{2\pi} (1-x)^{-re^{i\varphi}} \frac{re^{i\varphi}}{(1+re^{i\varphi})(2+re^{i\varphi})} \exp\left[-\frac{\alpha_s C_F}{\pi} \hat{a} \ln(re^{i\varphi})\right] \\
&\quad \left. + \int_{\ln r}^{+\infty} \frac{dw}{\pi} (1-x)^{e^w} \frac{e^w}{(1-e^w)(2-e^w)} \exp\left[-\frac{\alpha_s C_F}{\pi} \hat{a} w\right] \sin[\alpha_s C_F \hat{a}] \right\}, \quad (3.12)
\end{aligned}$$

for the variable

$$\hat{a} = \ln\left(\frac{\tilde{a}}{a} P^- b\right) > 0. \quad (3.13)$$

The first term in the above expression comes from the contributions of the $N = -1$ and -2 poles, the second term corresponds to the integration along the circle at $N = 0$ with radius r , and the last term arises from the discontinuity of the integrand along the branching cut. It can be verified that $\bar{\Phi}^I(x, b, \zeta_1^2, t)$ is independent of the radius $0 < r < 1$ as it should.

The inverse Mellin transformation is performed along the same line in the case of the flat model. The initial condition introduces only a single pole at $N = 0$, which is also a branching point of the exponential in Eq. (3.8). The contour is shown in Fig. 2, with the two infinitesimal circles around $N = -1$ and $= 2$ being removed. This immediately yields

$$\begin{aligned}
& \bar{\Phi}^{II}(x, b, \zeta_1^2, t) \\
&= \exp\left(-\frac{b^2}{4\beta^2}\right) \exp\left\{\frac{\alpha_s C_F}{\pi} \left[-2\hat{a} + \frac{3}{2} \ln\left(\frac{t}{\mu_i}\right)\right]\right\} \\
&\times \left\{ \int_{-\pi}^{\pi} \frac{d\varphi}{2\pi} (1-x)^{-re^{i\varphi}} \exp\left[-\frac{\alpha_s C_F}{\pi} \hat{a} \ln(re^{i\varphi})\right] \right. \\
&\quad \left. - \int_{\ln r}^{+\infty} \frac{dw}{\pi} (1-x)^{e^w} \exp\left[-\frac{\alpha_s C_F}{\pi} \hat{a} w\right] \sin[\alpha_s C_F \hat{a}] \right\}. \quad (3.14)
\end{aligned}$$

The resummation improved wave function with the initial condition $\tilde{\Phi}^{III}(N, b, \zeta_0^2, \mu_i)$ is calculated similarly, albeit with more involved analytical structures of the integrand; we need to modify the contour in Fig. 2, so that two additional poles at $N = -3$ and -4 are circumvented. It implies that including higher Gegenbauer terms in the initial condition of the wave function generates a longer sequence of poles to be avoided in the contour integration. We derive

$$\bar{\Phi}^{III}(x, b, \zeta_1^2, t)$$

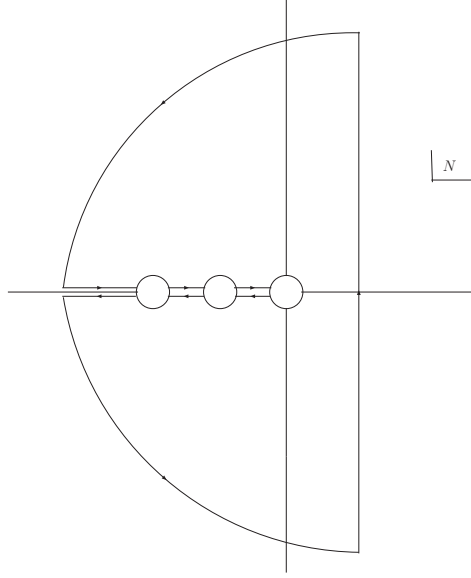


Figure 2: Integration contour of the inverse Mellin transformation for the asymptotic pion wave function. Two infinitesimal circles at $N = -1$ and -2 and a finite circle at $N = 0$ with radius r are introduced to ensure that the function $\tilde{\Phi}(N, b, \zeta_1^2, t)$ is analytical in the region embraced by the contour.

$$\begin{aligned}
&= 6 \exp\left(-\frac{b^2}{4\beta^2}\right) \exp\left\{\frac{\alpha_s C_F}{\pi} \left[-2\hat{a} + \frac{3}{2} \ln\left(\frac{t}{\mu_i}\right)\right]\right\} \\
&\times \left\{ \sum_{n=1}^4 \kappa_n (1-x)^n \exp[-\alpha_s C_F \hat{a} \ln n] \cos[\alpha_s C_F \hat{a}] \right. \\
&\quad + \int_{-\pi}^{\pi} \frac{d\varphi}{2\pi} (1-x)^{-re^{i\varphi}} \frac{r e^{i\varphi} f(a_2, r e^{i\varphi})}{(1+re^{i\varphi})(2+re^{i\varphi})} \exp\left[-\frac{\alpha_s C_F}{\pi} \hat{a} \ln(re^{i\varphi})\right] \\
&\quad \left. + \int_{\ln r}^{+\infty} \frac{dw}{\pi} (1-x)^{e^w} \frac{e^w f(a_2, -e^w)}{(1-e^w)(2-e^w)} \exp\left[-\frac{\alpha_s C_F}{\pi} \hat{a} w\right] \sin[\alpha_s C_F \hat{a}] \right\}, \tag{3.15}
\end{aligned}$$

where the coefficients κ_n and the function $f(x_1, x_2)$ are given by

$$\begin{aligned}
\kappa_1 &= 1 + 6a_2, & \kappa_2 &= -(1 + 36a_2), \\
\kappa_3 &= 60a_2, & \kappa_4 &= -30a_2, \\
f(x_1, x_2) &= 1 + 6x_1 \frac{(-1+x_2)(-2+x_2)}{(3+x_2)(4+x_2)}. \tag{3.16}
\end{aligned}$$

Apparently, Eq. (3.15) reduces to Eq. (3.12), when the second Gegenbauer moment a_2 is set to zero.

A more complicated model for the pion wave function

$$\phi^{\text{IV}}(x, \zeta_0^2, \mu_i) = \frac{\Gamma(2 + 2\alpha)}{[\Gamma(1 + \alpha)]^2} (x\bar{x})^\alpha, \quad (3.17)$$

with $0 < \alpha < 1$, has been advocated in [40]. The corresponding initial condition

$$\tilde{\Phi}^{\text{IV}}(N, b, \zeta_0^2, \mu_i) = \frac{\Gamma(2 + 2\alpha)}{[\Gamma(1 + \alpha)]^2} \frac{\Gamma(N + \alpha)}{\Gamma(N + 2\alpha + 1)} \exp\left(-\frac{b^2}{4\beta^2}\right), \quad (3.18)$$

develops infinitely many poles at $N + \alpha = 0, -1, -2, \dots$ in the complex N plane. The study of the joint-resummation effect on this model is similar, and will not be repeated here.

3.2 Resummation with running α_s

We are now in a position of computing the joint-resummation improved pion wave function $\bar{\Phi}(x, b, \zeta_1^2, t)$ with a running coupling α_s . To avoid the Landau singularity in the inverse Mellin transformation, the parametrization [41]

$$\alpha_s(\mu) = \frac{4\pi}{\beta_0} \left[\frac{1}{\ln(\mu^2/\Lambda_{\text{QCD}}^2)} - \frac{\Lambda_{\text{QCD}}^2}{\mu^2 - \Lambda_{\text{QCD}}^2} \right], \quad (3.19)$$

is adopted at one loop, with the QCD scale Λ_{QCD} and the one-loop QCD β function $\beta_0 = (11N_c - 2N_f)/3$ is, N_c and N_f being the numbers of colors and flavors, respectively. In the above expression the first term preserves the ultraviolet behavior of the standard QCD coupling, and the second term cancels the ghost pole at $\mu = \Lambda_{\text{QCD}}$.

The substitution of Eq. (3.19) into Eq. (2.32) produces

$$\tilde{\Phi}(N, b, \zeta_1^2, t) = \exp\left[\frac{C_F}{\beta_0}(A_1 + C_1)\right] \tilde{\Phi}(N, b, \zeta_0^2, \mu_i), \quad (3.20)$$

where the functions A_1 and C_1 are written as

$$\begin{aligned} A_1 &= \sum_{i=1}^4 (-1)^{n-1} [r_i(\ln r_i - 1) - \text{Li}_2(e^{-r_i})], \\ C_1 &= 3 \left[\ln \frac{1 - \Lambda_{\text{QCD}}^2/\mu_i^2}{1 - \Lambda_{\text{QCD}}^2/t^2} + \ln \frac{\ln(t^2/\Lambda_{\text{QCD}}^2)}{\ln(\mu_i^2/\Lambda_{\text{QCD}}^2)} \right], \end{aligned} \quad (3.21)$$

with the parameters

$$\begin{aligned} r_{1(3)} &= \frac{1}{2} \ln N + \lambda_{1(3)}, & r_{2(4)} &= -\frac{3}{2} \ln N + \lambda_{2(4)}, \\ \lambda_{1(3)} &= \lambda_{2(4)} + 4, & \lambda_2 &= 2 \ln \frac{2a}{\Lambda_{\text{QCD}} b}, & \lambda_4 &= 2 \ln \frac{2\tilde{a}P^-}{\Lambda_{\text{QCD}}}. \end{aligned}$$

The exponential in Eq. (3.20) still contains a branching cut along the negative real N axis, so the contour in Eq. (3.1) is deformed in the way exactly the same as in the case with a frozen coupling.

For the asymptotic pion wave function, we get

$$\begin{aligned}
& \overline{\Phi}^{\text{I}}(x, b, \zeta^2, t) \\
&= 6 \exp\left(-\frac{b^2}{4\beta^2}\right) \exp\left(\frac{C_F}{\beta_0} C_1\right) \\
&\times \left\{ \sum_{n=1}^2 (-1)^{n-1} (1-x)^n \exp\left[F_1(\lambda_1, \lambda_2, \lambda_3, \lambda_4, n)\right] \cos\left[F_2(\lambda_1, \lambda_2, \lambda_3, \lambda_4, n)\right] \right. \\
&\quad + \int_{-\pi}^{\pi} \frac{d\varphi}{2\pi} (1-x)^{-re^{i\varphi}} \frac{re^{i\varphi}}{(1+re^{i\varphi})(2+re^{i\varphi})} \exp\left[F_3(\lambda_1, \lambda_2, \lambda_3, \lambda_4, re^{i\varphi})\right] \\
&\quad - \int_{\ln r}^{+\infty} \frac{dw}{\pi} (1-x)^{e^w} \frac{e^w}{(1-e^w)(2-e^w)} \exp\left[F_1(\lambda_1, \lambda_2, \lambda_3, \lambda_4, e^w)\right] \\
&\quad \left. \times \sin\left[F_2(\lambda_1, \lambda_2, \lambda_3, \lambda_4, e^w)\right] \right\}, \tag{3.22}
\end{aligned}$$

where the explicit expressions of the functions $F_i(\lambda_1, \lambda_2, \lambda_3, \lambda_4, \eta)$ are collected in Appendix A, and the discontinuity of the polylogarithm function

$$\text{Im} [\text{Li}_2(z \pm i\epsilon)] = \mp \pi \ln z \theta(z - 1), \tag{3.23}$$

has been inserted. It has been also verified that the r dependence of $\overline{\Phi}^{\text{I}}(x, b, \zeta_1^2, t)$ cancels between the last two terms for arbitrary $0 < r < 1$ as expected.

The same procedure leads to the joint-resummation improved pion wave function

$$\begin{aligned}
& \overline{\Phi}^{\text{II}}(x, b, \zeta_1^2, t) = \exp\left(-\frac{b^2}{4\beta^2}\right) \exp\left(\frac{C_F}{\beta_0} C_1\right) \\
&\times \left\{ \int_{-\pi}^{\pi} \frac{d\varphi}{2\pi} (1-x)^{-re^{i\varphi}} \exp\left[F_3(\lambda_1, \lambda_2, \lambda_3, \lambda_4, re^{i\varphi})\right] \right. \\
&\quad + \int_{\ln r}^{+\infty} \frac{dw}{\pi} (1-x)^{e^w} \exp\left[F_1(\lambda_1, \lambda_2, \lambda_3, \lambda_4, e^w)\right] \\
&\quad \left. \times \sin\left[F_2(\lambda_1, \lambda_2, \lambda_3, \lambda_4, e^w)\right] \right\}, \tag{3.24}
\end{aligned}$$

for the flat model, and

$$\begin{aligned}
& \overline{\Phi}^{\text{III}}(x, b, \zeta_1^2, t) \\
&= 6 \exp\left(-\frac{b^2}{4\beta^2}\right) \exp\left(\frac{C_F}{\beta_0} C_1\right) \\
&\times \left\{ \sum_{n=1}^4 \kappa_n (1-x)^n \exp\left[F_1(\lambda_1, \lambda_2, \lambda_3, \lambda_4, n)\right] \cos\left[F_2(\lambda_1, \lambda_2, \lambda_3, \lambda_4, n)\right] \right\}
\end{aligned}$$

$$\begin{aligned}
& + \int_{-\pi}^{\pi} \frac{d\varphi}{2\pi} (1-x)^{-re^{i\varphi}} \frac{re^{i\varphi}}{(1+re^{i\varphi})(2+re^{i\varphi})} \exp \left[F_3(\lambda_1, \lambda_2, \lambda_3, \lambda_4, re^{i\varphi}) \right] \\
& \times \left[1 + 6a_2 \frac{(-1+re^{i\varphi})(-2+re^{i\varphi})}{(3+re^{i\varphi})(4+re^{i\varphi})} \right] \\
& - \int_{\ln r}^{+\infty} \frac{dw}{\pi} (1-x)^{e^w} \frac{e^w}{(1-e^w)(2-e^w)} \left[1 + 6a_2 \frac{(-1-e^w)(-2-e^w)}{(3-e^w)(4-e^w)} \right] \\
& \times \exp \left[F_1(\lambda_1, \lambda_2, \lambda_3, \lambda_4, e^w) \right] \sin \left[F_2(\lambda_1, \lambda_2, \lambda_3, \lambda_4, e^w) \right] \Big\}, \tag{3.25}
\end{aligned}$$

for the non-asymptotic model.

The joint-resummation effect on the pion wave function with a frozen coupling, for the example set parameters $\alpha_s = 0.3$, $b = 2\tilde{a}P^-/a$ and $4\tilde{a}P^-/a$, and $Q^2 = 5 \text{ GeV}^2$ is displayed in Fig. 3, where the RG evolution effect is not included. For all the three considered models, the modification appears as the impact parameter b is greater than $b_{\min} = \tilde{a}/(aP^-)$, which is easily understood from the exponentiation of the mixed logarithm $-\ln(\tilde{a}P^-b/a)(\ln N + 2)$ in Eq. (3.8). If the rapidity and factorization-scale evolutions are switched off, it is confirmed that the pion wave function obeys its normalization. A crucial consequence of the joint resummation, as read from Fig. 3, is that the small x region receives stronger suppression compared to the moderate x region as expected, while the large x region almost remains intact. Moreover, the suppression strengthens with the transverse separation b between the valence quarks at a given longitudinal momentum fraction. Therefore, the joint-resummation effect does not allow a significant contribution from soft gluon exchanges. This well known Sudakov mechanism, first formulated in QED, improves the applicability of PQCD to hard exclusive processes.

Turning to the case with a running coupling, we adopt the parameter $\Lambda_{\text{QCD}} = 250 \text{ MeV}$ and the flavor number $N_f = 6$. As observed from Fig. 3, the resummation improved pion wave function takes on a behavior rather similar to that for a frozen coupling. A minor difference is that the small x region is even more suppressed in the former case, which further boosts our confidence on the applicability of PQCD to exclusive processes at moderate momentum transfer.

Before closing this section, we highlight the distinction between the pion wave functions including the Sudakov resummation and including the joint resummation. For simplicity, we confine ourselves to the asymptotic model, because the other two models exhibit a similar b dependence. As displayed in Fig. 4, both resummation formalisms lead to suppression on the wave function in the large b region, which becomes more significant as the momentum transfer Q increases. This observation fulfills the concept that an energetic pion is a compact hadronic bound state. A striking feature is that the joint-resummation improved wave function concentrates on the small b region more than the Sudakov-resummation improved one, which falls off smoothly in the intermediate b region. The concentration on the small b region is attributed to the exponentiation of the mixed logarithm $-\ln(\tilde{a}P^-b/a)\ln N$, where the suppression with b is magnified by the large coefficient $\ln N$. However, the Sudakov-resummation improved wave function vanishes quickly as $b \rightarrow 1/\Lambda_{\text{QCD}}$, since the

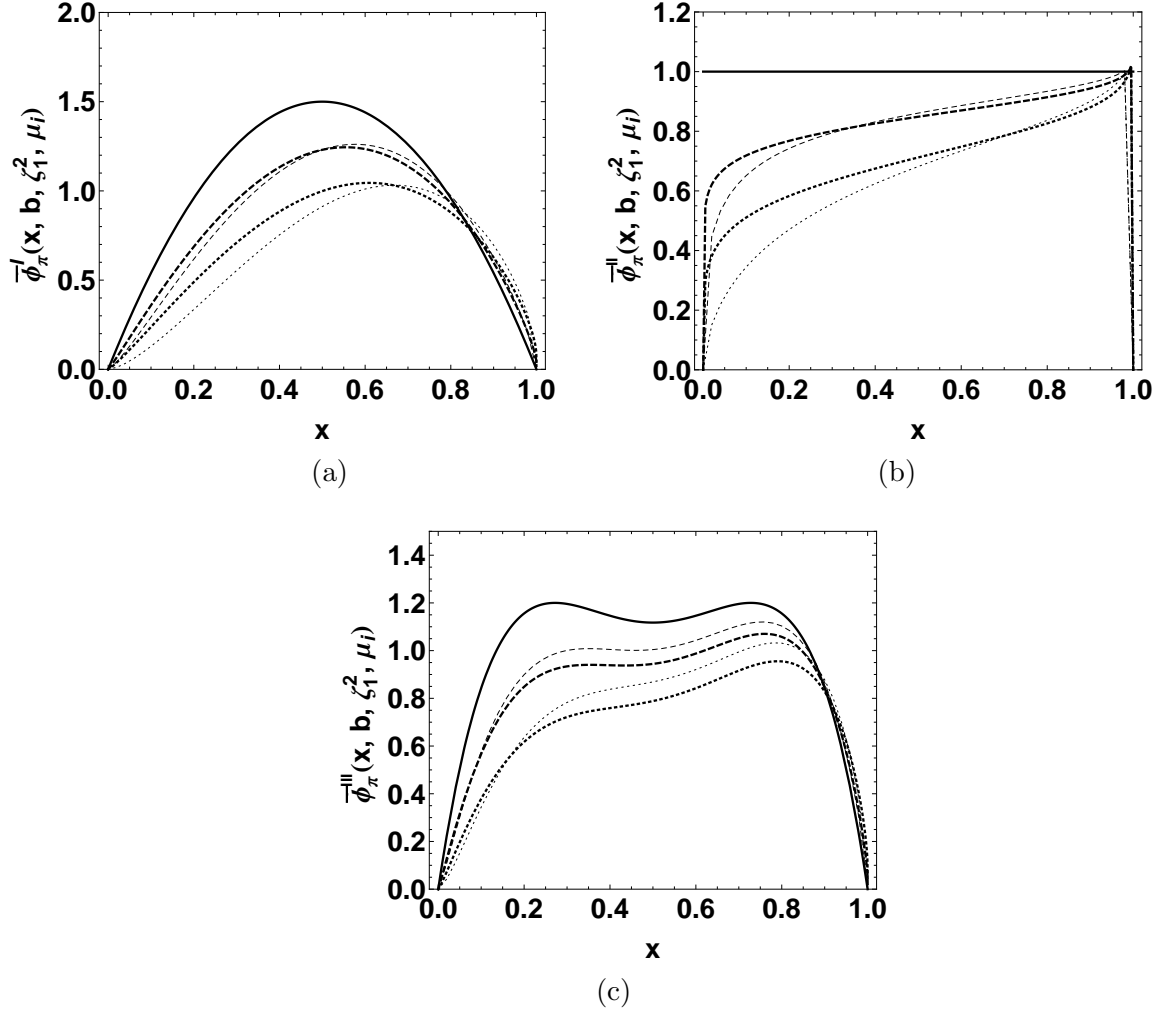


Figure 3: Shape of the pion wave function in different models. (a) the solid, (thin) dashed and (thin) dotted curves correspond to the initial condition $\phi^I(x, \zeta_0^2, \mu_i)$, the joint-resummation improved wave function $\bar{\Phi}^I(x, 2\tilde{a}P^-/a, \zeta_1^2, \mu_i)$ and $\bar{\Phi}^I(x, 4\tilde{a}P^-/a, \zeta_1^2, \mu_i)$ for a frozen $\alpha_s = 0.3$ (running α_s). (b) the same for the flat pion wave function $\bar{\Phi}^{II}(x, b, \zeta_1^2, \mu_i)$. (c) the same for the non-asymptotic pion wave function $\bar{\Phi}^{III}(x, b, \zeta_1^2, \mu_i)$ with the second Gegenbauer moment $a_2 = 0.17$ determined in [42].

running coupling $\alpha_s(1/b)$ hits the Landau pole. In the present derivation the Landau pole has been avoided as shown in Eq. (3.19), such that the joint resummation does not diminish the wave function as $b \rightarrow 1/\Lambda_{\text{QCD}}$. We emphasize that this distinction, due to the different treatments of the Landau-pole contribution, is not physically crucial. It is found that the large b region is more suppressed with the growing of x in Figs. 4(b), but not in Fig. 4(d): the small- x approximation has been adopted in the joint resummation, so its effect is insensitive to the variation of x . The phenomenological consequences on the pion transition form factor from the two resummations will be elaborated in the next section.

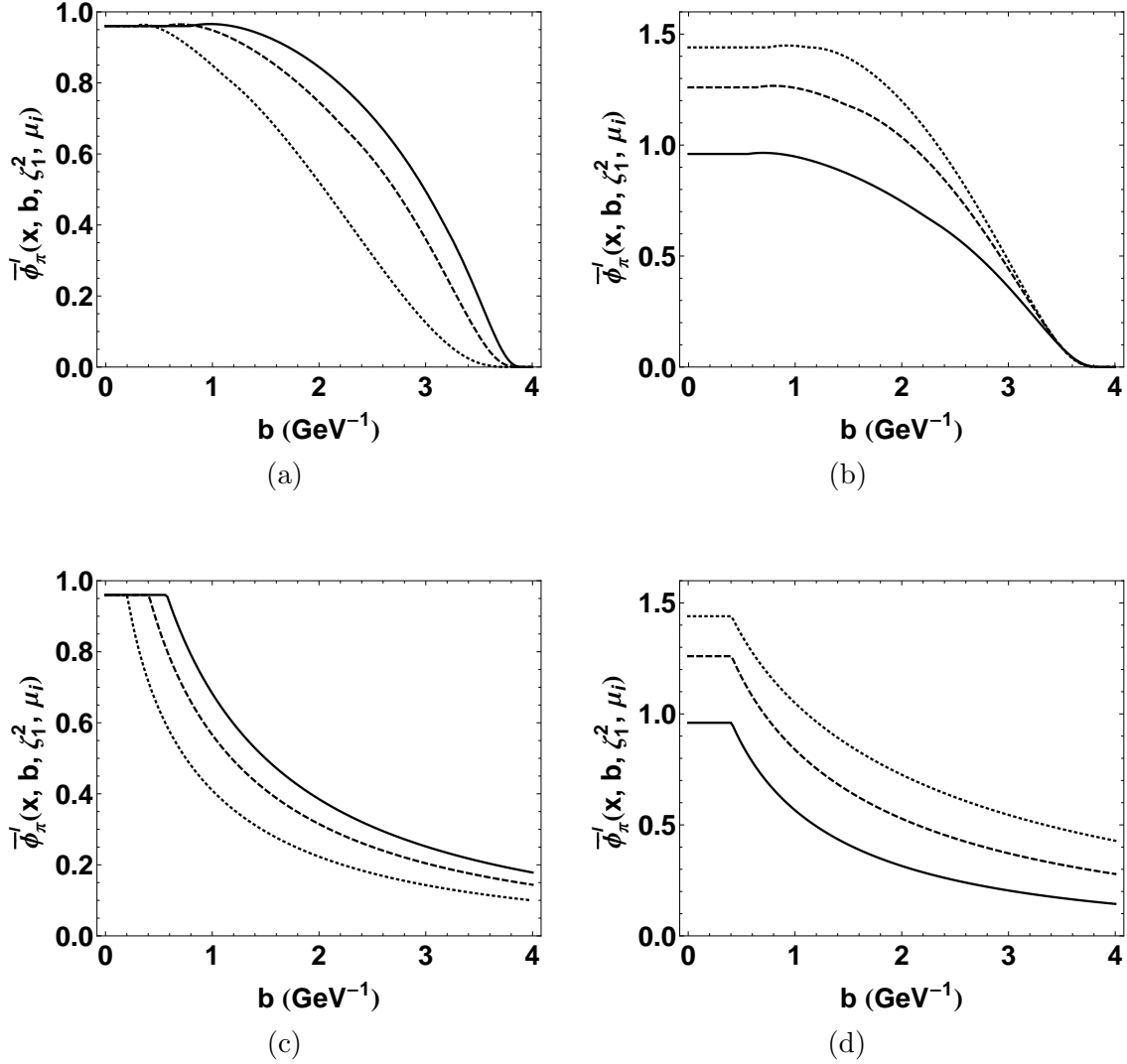


Figure 4: Distinction between the asymptotic pion wave functions including the Sudakov resummation and including the joint resummation. The solid, dashed, and dotted curves correspond to the Sudakov-resummation improved pion wave function () at $Q^2 = 5$ GeV 2 , 10 GeV 2 , and 40 GeV 2 for the momentum fraction $x = 0.2$, and (b) at $Q^2 = 10$ GeV 2 for $x = 0.2, 0.3$, and 0.4 . The same for the joint-resummation improved pion wave functions in (c) and (d).

4. PION TRANSITION FORM FACTOR

The pion transition form factor $F(Q^2)$ involved in the $\gamma^* \pi^0 \rightarrow \gamma$ process is defined by the following matrix element

$$\langle \gamma(P', \epsilon^*) | j_\mu^{em}(q) | \pi^0(P) \rangle = i g_{em}^2 \epsilon_{\mu\nu\alpha\beta} \epsilon^{*\nu} P^\alpha P'^\beta F(Q^2), \quad (4.1)$$

where $j_\mu^{em}(q)$ is an electromagnetic current, $q = P' - P$ is the momentum transfer, and ϵ denotes the polarization of the outgoing photon. The form factor $F(Q^2)$ ($Q^2 = -q^2$) was

written, in the collinear factorization, as [35]

$$F(Q^2) = \frac{\sqrt{2} f_\pi}{3} \int_0^1 dx \frac{\varphi(x, t)}{x Q^2} \left[1 + H^{(1)}(x, Q^2, t) \right], \quad (4.2)$$

with the NLO hard kernel [43, 44, 45]

$$H^{(1)}(x, Q^2, t) = \frac{\alpha_s(t) C_F}{2\pi} \left[- \left(\ln x + \frac{3}{2} \right) \ln \frac{t^2}{Q^2} + \frac{1}{2} \ln^2 x - \frac{x \ln x}{2(1-x)} - \frac{9}{2} \right]. \quad (4.3)$$

It is seen that $F(Q^2)$ scales as $1/Q^2$ from the power counting of the hard kernel, and is determined by the inverse moment of the pion LCDA at LO.

4.1 k_T factorization formula

To suppress the end-point contribution (soft gluon exchanges) from the small x region in the collinear factorization, the k_T factorization has been developed for hard exclusive processes, and continually refined by including the resummations of important logarithms and power corrections as stated in the Introduction. This more sophisticated factorization theorem can be derived diagrammatically [46] by applying the eikonal approximation to collinear particles and the Ward identity to the diagram summation in the leading infrared regions. For the rapidity parameter $\zeta^2 = 2$, the k_T factorization formula at leading power of $1/Q^2$ under the conventional resummations was given by [7, 26]

$$F(Q^2) = \frac{\sqrt{2} f_\pi}{3} \int_0^1 dx \int_0^\infty b db \bar{\Phi}(x, b, t) e^{-S(x, b, Q, t)} S_t(x, Q) \\ \times K_0(\sqrt{x} Q b) \left[1 - \frac{\alpha_s(t) C_F}{4\pi} \left(3 \ln \frac{t^2 b}{2\sqrt{x} Q} + \gamma_E + 2 \ln x + 3 - \frac{\pi^2}{3} \right) \right]. \quad (4.4)$$

The Sudakov factor $S(x, b, Q, t)$ sums the double logarithm $\ln^2(k_T^2/Q^2)$ and the single logarithm $\ln(t^2/Q^2)$ through the RG equation. The threshold factor from the resummation of $\ln^2 x$ has been parameterized as

$$S_t(x, Q) = \frac{2^{1+c(Q^2)} \Gamma(\frac{3}{2} + c(Q^2))}{\sqrt{\pi} \Gamma(1 + c(Q^2))} [x(1-x)]^{c(Q^2)}, \quad (4.5)$$

for convenience, in which the power $c(Q^2)$ is determined to be

$$c(Q^2) = 0.04Q^2 - 0.51Q + 1.87, \quad (4.6)$$

by fitting to the exact threshold resummation formula in the Mellin space. It was then observed that the nontrivial Q^2 dependence of $c(Q^2)$ is important for accommodating both low and high Q^2 data from BaBar. Note that the self interactions of the Wilson links have been included into the NLO hard kernel in Eq. (4.4), such that the coefficient of the first term in the brackets has been changed from “1” to “3”, compared to Eq. (40) in [7]. As argued in [47], the additional contribution from these self interactions can be canceled by the soft subtraction in an alternative definition for the TMD pion wave function, as

the involved gauge parameter is tuned appropriately. In this work we have adopted the definition of the TMD pion wave function with off light-cone Wilson links.

To minimize the factorization-scheme dependence of the pion transition form factor, the resummation of the mixed logarithm $\ln x \ln(\zeta^2 P^{-2}/k_T^2)$ in both the pion wave function and the hard kernel has been performed in the previous section. The large logarithms in the initial conditions of the pion wave function and the hard kernel were eliminated by choosing the bounds ζ_0^2 and ζ_1^2 in Eqs. (2.32) and (2.36), leading to

$$H^{(1)}(x, k_T, \zeta_1^2, Q^2, t) = -\frac{\alpha_s(t)C_F}{4\pi} \left(3 \ln \frac{t^2}{xQ^2 + k_T^2} + \ln 2 + 2 \right). \quad (4.7)$$

We then arrive at the joint-resummation improved factorization formula for the pion transition form factor

$$F(Q^2) = \frac{\sqrt{2}f_\pi}{3} \int_0^1 dx \int_0^\infty b db \bar{\Phi}(x, b, \zeta_1^2, t) K_0(\sqrt{x}Qb) \\ \times \left[1 - \frac{\alpha_s(t)C_F}{4\pi} \left(3 \ln \frac{t^2 b}{2\sqrt{x}Q} + \ln 2 + 2 \right) \right], \quad (4.8)$$

with $\bar{\Phi}(x, b, \zeta_1^2, t)$ coming from Eqs. (3.22), (3.24), and (3.25).

4.2 Numerical analysis

The first issue in the numerical analysis concerns the choice of the hard characteristic scale t . One choice would be $t^2 = \sqrt{x}Q/b$ that removes the remaining logarithm in Eq. (4.8). With this scenario the hard scale may run into the nonperturbative region or the rather high energy region, depending on the competition of the momentum fraction x and the transverse separation b . Another choice characterizing the typical quantum fluctuation of hard scattering is $t = \max(\sqrt{x}Q, 1/b)$ as widely adopted in the PQCD approach [5]. We have confirmed that the two choices of the hard scale do not generate practical difference in our formalism for the pion transition form factor. It implies that the joint resummation has suppressed the contribution from the nonperturbative region effectively. Below we will take the second scenario as the default choice.

Another important issue is the determination of the Gegenbauer moment a_2 . QCDSR calculations of moments of the pion wave function can be traced back to 1980s, pioneered by Chernyak and Zhitnitsky [48], where a rather high value $a_2(\mu) \sim 0.58$ at the scale $\mu^2 \in [1, 2] \text{ GeV}^2$ was derived. This estimate was improved gradually by including NLO QCD corrections and refining the “internal” parameters of the QCDSR approach. The most recent update gave $a_2(1 \text{ GeV}) = 0.15 \pm 0.03$ [49]. Following the strategy of light-cone sum rules (LCSR), we will not use the Gegenbauer coefficient a_2 computed from QCDSR directly. Instead, we adopt the value [42]

$$a_2(1 \text{ GeV}) = 0.17 \pm 0.08, \quad (4.9)$$

extracted from matching the LCSR calculation of the pion electromagnetic form factor, which includes NLO twist-2 corrections and higher power terms up to twist 6, to the experimental data from the Jefferson Lab Collaboration.

We start our numerical analysis by considering the asymptotic pion wave function. As observed from Fig. 5(a), the predicted $Q^2 F(Q^2)$ with the conventional resummations at both LO and NLO levels saturates rapidly as $Q^2 > 5 \text{ GeV}^2$, and the NLO QCD correction enhances the form factor by (6–14)%. It is clear that the asymptotic pion distribution generally accommodates the Belle data except the first two bins. However, it cannot describe the CLEO-c and BaBar data in both small and large Q^2 region. The joint-resummation effect decreases the LO and NLO predictions in the conventional approach by (11–16)% and (8–27)%, respectively. Such decrease can be understood via the stronger reduction in the small x region from the joint resummation as shown in Figs. 4(b) and 4(d), which is the dominant region owing to the hard kernel $K_0(\sqrt{x}Qb)$. It is found that the saturation behavior of $Q^2 F(Q^2)$ changes slightly at NLO in the joint-resummation improved k_T factorization: the NLO correction brings about 6% suppression (15% enhancement) to the LO result in the small (large) Q^2 region. The above decrease of the NLO form factor at small Q^2 is explained as follows. The contribution to the pion transition form factor under the joint resummation mainly comes from the small b region as indicated by Fig. 4. We then have $t^2 b \sim 1/b > \sqrt{x}Q$ at small Q , for which the logarithm of the NLO hard kernel in Eq. (4.8) flips sign. The failure of describing the experimental data suggests that the pion wave function might be broader. This observation is in agreement with the particular feature of the pion as a Nambu-Goldstone boson of dynamical chiral symmetry breaking and with the recent lattice simulations [40].

The computed pion transition form factor $Q^2 F(Q^2)$ with the flat pion wave function is shown in Fig. 5(b). It is seen that the form factor grows steadily with Q^2 at LO and NLO under both resummation formalisms. This is easily realized from the scaling $Q^2 F(Q^2) \sim \ln(Q^2/k_T^2)$ implied by the tree-level k_T factorization formula with the flat pion wave function [26]. The NLO correction enhances the form factor by approximately (15–18)% in the convention approach, and reasonably describes the scaling violation at large Q^2 observed by BaBar and the low Q^2 data from CLEO-c. Compared to the conventional approach, the predictions from the joint resummation brings about 17% enhancement and (8–16)% suppression at the LO and NLO levels, respectively. Note that the NLO correction becomes destructive under the joint resummation in the whole range of Q^2 , decreasing the LO result by (10–15)%. This behavior, different from that in the case of the asymptotic pion wave function, is also traced back to the logarithmic term in Eq. (4.8): $\ln(t^2 b/(\sqrt{x}Q))$ remains positive in the small x region, which is probed more by the flat pion wave function.

The input of the third model of the pion wave function with a nonvanishing second Gegenbauer moment a_2 leads to the predicted $Q^2 F(Q^2)$ displayed in Fig. 5(c). The form factor under the conventional resummations behaves in a way similar to that in Fig. 5(a): $Q^2 F(Q^2)$ exhibits saturation as $Q^2 > 10 \text{ GeV}^2$, and the magnitude is larger; namely, it goes between the BaBar and Belle data. These features are attributed to the broader pion wave function, which enhances the small- x contribution. Note that the joint resummation also modifies the normalization of the pion wave function, such that the model with a finite a_2 may be higher than the flat model in the small- x region, say, in $0.1 < x < 0.2$. This explains why the curve for $Q^2 F(Q^2)$ under the joint resummation ascends fastest with Q^2 here. Compared with the form factor in the conventional approach, it shows (4–18)%

enhancement at LO and $(13 - 32)\%$ correction at NLO. It is evident that the BaBar data can be excellently described by the joint-resummation improved factorization and the pion wave function with a nonvanishing a_2 , particularly in the large Q^2 region.

In summary, the significance of the NLO contribution and the saturation behavior of the pion transition form factor are quite different under the joint resummation and the conventional resummations. This observation indicates the importance of appropriate treatment of QCD logarithmic corrections to a process. It is also crucial to clarify the high Q^2 data of the pion transition form factor on the experimental side, in order to acquire better understanding of the hadron structure and stringent scrutinization of perturbation theory.

To illustrate theoretical uncertainties, we vary the default choice of the hard scale by a factor of 2, namely, $t = \max(2\sqrt{x}Q, 1/b)$. As shown in Fig. 6, the scale variation increases the pion transition form factor in the large Q^2 region by approximately 8% and 1% at LO and NLO, respectively, for the asymptotic pion wave function. On the other hand, tuning the hard scale magnifies the QCD correction, as large as 7%, to the pion transition form factor in the flat model. This is certainly not unexpected, taking into account the highlighted role of the single logarithm $\ln(t^2 b/(\sqrt{x}Q))$ in the hard kernel. Similar observation also holds for the non-asymptotic model with a finite a_2 , albeit with the NLO correction being enhanced to 13% at NLO.

5. CONCLUSION AND DISCUSSION

Applying the resummation technique with off-light-cone Wilson lines, we have constructed an evolution equation to resum the mixed logarithm $\ln x \ln(\zeta_P^2/k_T^2)$ in the TMD pion wave function. The joint-resummation improved pion wave function modifies both the longitudinal and transverse momentum distributions. As a consequence, both the small x and b regions are more highlighted compared to the case with the conventional threshold and k_T resummations. We stress that the joint resummation, organizing all the important logarithms in the pion wave function and in the hard kernel, is a treatment more appropriate and complete than the conventional resummations. In particular, Eq. (4.8) derived in this work represents the first scheme-independent k_T factorization formula for the pion transition form factor in the presence of the light-cone singularity.

We have examined the significance of the NLO contribution and the saturation behavior of the pion transition form factor at high energy under the joint resummation. Differences from those under the conventional resummations were noticed, indicating that QCD logarithmic corrections to a process must be handled appropriately, before its data are used to extract a hadron wave function. Our predictions for the pion transition form factor have been confronted with the measurements from CLEO, BaBar and Belle by testing three models for the pion wave function. The comparison shows that the asymptotic pion wave function fails to describe the data in both small and large Q^2 regions, even after the factorization scale was varied by a factor of two. The predictions from the joint-resummation improved factorization formula with the flat pion wave function and with the hard scale widely chosen in the PQCD approach balance the BaBar and Belle data well.

Including the first-order non-asymptotic correction to the pion wave function, we found that the resultant pion transition form factor matches the BaBar data at the large momentum transfer. Resolving the discrepancy between the BaBar and Belle measurements will definitely improve our understanding towards the hadronic structure of a pion.

Our scheme-independent formalism can be extended to the k_T factorization of more complicated exclusive processes. We will demonstrate this extension taking the pion electromagnetic form factor as an example. The first step is to verify that the choice of ζ_0^2 , with N and b being replaced by $N_{1(2)}$ and $b_{1(2)}$ for the incoming (outgoing) pion, defined in Eq. (2.37) diminishes the large logarithms in the NLO TMD pion wave function in Eq. (33) of [8]. It is indeed the case under the power counting $k_{1T}^2 \sim k_{2T}^2 \sim x_1 x_2 Q^2$, confirming the universality of a TMD hadron wave function. To eliminate the large logarithms in the hard kernel given by Eq. (35) of [8], we may set

$$\zeta_1^2 = N_2^{-45/8} N_1^{1/2}, \quad \zeta_2^2 = N_1^{-45/8} N_2^{1/2},$$

which arise from the simultaneous solution to the evolution equations for two TMD pion wave functions and one hard kernel. The remaining single logarithms in the hard kernel can be further removed by choosing the factorization scale μ_f that satisfies the constraint

$$6 \ln \frac{\mu_f^2}{Q^2} + \frac{8}{27} \ln x_1 - \frac{3}{16} \ln x_2 = 0.$$

We will present the details of the joint-resummation improved factorization for the pion electromagnetic form factor elsewhere.

Acknowledgement

HNL is supported in part by the National Science Council of R.O.C. under Grant No. NSC-101-2112-M-001-006-MY3, and by the National Center for Theoretical Sciences of R.O.C.. YLS acknowledges the support of National Science Foundation of China under Grant No. 11005100. YMW is supported by the DFG Sonderforschungsbereich /Transregio 9 ‘‘Computergestutzte Theoretische Teilchenphysik’’.

A. Explicit expressions of the functions F_i

The functions $F_i(\lambda_1, \lambda_2, \lambda_3, \lambda_4, \eta)$ ($i = 1, 2, 3$) appearing in the joint-resummation improved pion wave function $\overline{\Phi}^{(\text{I,II,III})}(x, b, \zeta_1^2, t)$ in Eqs. (3.22), (3.24), and (3.25) are defined as

$$\begin{aligned} & F_1(\lambda_1, \lambda_2, \lambda_3, \lambda_4, \eta) \\ &= \frac{C_F}{\beta_0} \left\{ \hat{\lambda}_1 \left[\frac{1}{2} \ln \left(\hat{\lambda}_1^2 + \frac{\pi^2}{4} \right) - 1 \right] - \frac{\pi}{2} \theta_1(\lambda_1, \eta) - \hat{\lambda}_2 \left[\frac{1}{2} \ln \left(\hat{\lambda}_2^2 + \frac{9\pi^2}{4} \right) - 1 \right] - \frac{3\pi}{2} \theta_2(\lambda_2, \eta) \right. \\ & \quad - \hat{\lambda}_3 \left[\frac{1}{2} \ln \left(\hat{\lambda}_3^2 + \frac{\pi^2}{4} \right) - 1 \right] + \frac{\pi}{2} \theta_3(\lambda_3, \eta) + \hat{\lambda}_4 \left[\frac{1}{2} \ln \left(\hat{\lambda}_4^2 + \frac{9\pi^2}{4} \right) - 1 \right] + \frac{3\pi}{2} \theta_4(\lambda_4, \eta) \\ & \quad \left. - \frac{1}{4} \text{Li}_2 \left(-e^{-2\hat{\lambda}_1} \right) + \frac{1}{4} \text{Li}_2 \left(-e^{-2\hat{\lambda}_2} \right) + \frac{1}{4} \text{Li}_2 \left(-e^{-2\hat{\lambda}_3} \right) - \frac{1}{4} \text{Li}_2 \left(-e^{-2\hat{\lambda}_4} \right) \right\}, \quad (\text{A.1}) \end{aligned}$$

$$\begin{aligned}
& F_2(\lambda_1, \lambda_2, \lambda_3, \lambda_4, \eta) \\
&= \frac{C_F}{\beta_0} \left\{ \hat{\lambda}_1 \theta_1(\lambda_1, \eta) + \frac{\pi}{4} \ln \left(\hat{\lambda}_1^2 + \frac{\pi^2}{4} \right) - \hat{\lambda}_2 \theta_2(\lambda_2, \eta) + \frac{3\pi}{4} \ln \left(\hat{\lambda}_2^2 + \frac{9\pi^2}{4} \right) \right. \\
&\quad - \hat{\lambda}_3 \theta_3(\lambda_3, \eta) - \frac{\pi}{4} \ln \left(\hat{\lambda}_3^2 + \frac{\pi^2}{4} \right) + \hat{\lambda}_4 \theta_4(\lambda_4, \eta) - \frac{3\pi}{4} \ln \left(\hat{\lambda}_4^2 + \frac{9\pi^2}{4} \right) \\
&\quad \left. + \text{Im} \left[\text{Li}_2 \left(ie^{-\hat{\lambda}_1} \right) - \text{Li}_2 \left(ie^{-\hat{\lambda}_2} \right) - \text{Li}_2 \left(ie^{-\hat{\lambda}_3} \right) + \text{Li}_2 \left(ie^{-\hat{\lambda}_4} \right) \right] \right\}. \tag{A.2}
\end{aligned}$$

$$\begin{aligned}
& F_3(\lambda_1, \lambda_2, \lambda_3, \lambda_4, \eta) \\
&= \frac{C_F}{\beta_0} \left\{ \hat{\lambda}_1 \left(\ln \hat{\lambda}_1 - 1 \right) - \hat{\lambda}_2 \left(\ln \hat{\lambda}_2 - 1 \right) - \hat{\lambda}_3 \left(\ln \hat{\lambda}_3 - 1 \right) + \hat{\lambda}_4 \left(\ln \hat{\lambda}_4 - 1 \right) \right. \\
&\quad \left. - \text{Li}_2 \left(e^{-\hat{\lambda}_1} \right) + \text{Li}_2 \left(e^{-\hat{\lambda}_2} \right) + \text{Li}_2 \left(e^{-\hat{\lambda}_3} \right) - \text{Li}_2 \left(e^{-\hat{\lambda}_4} \right) \right\}, \tag{A.3}
\end{aligned}$$

with the short-hand notations $\hat{\lambda}_i$ and $\theta_i(\lambda_i, \eta)$

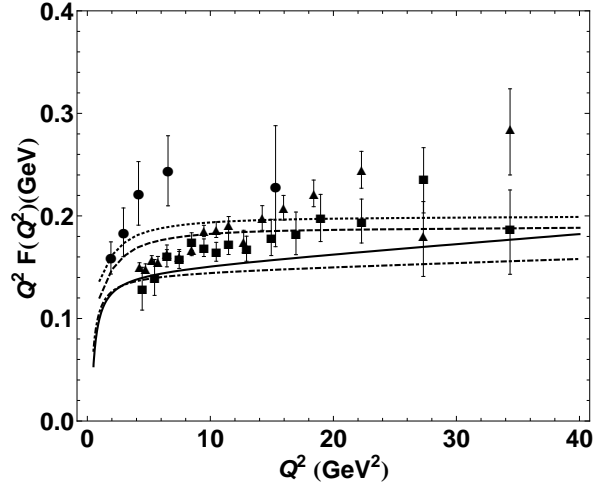
$$\begin{aligned}
\hat{\lambda}_{1(3)} &= \lambda_{1(3)} + \frac{1}{2} \ln \eta, & \hat{\lambda}_{2(4)} &= \lambda_{2(4)} - \frac{3}{2} \ln \eta, \\
\theta_1(\lambda_1, \eta) &= \arctan \left(\frac{\pi}{2\hat{\lambda}_1} \right) + \pi \theta \left(-\hat{\lambda}_1 \right), & \theta_2(\lambda_2, \eta) &= -\arctan \left(\frac{3\pi}{2\hat{\lambda}_2} \right) - \pi \theta \left(-\hat{\lambda}_2 \right), \\
\theta_3(\lambda_3, \eta) &= \theta_1(\lambda_3, \eta), & \theta_4(\lambda_4, \eta) &= \theta_2(\lambda_4, \eta).
\end{aligned}$$

References

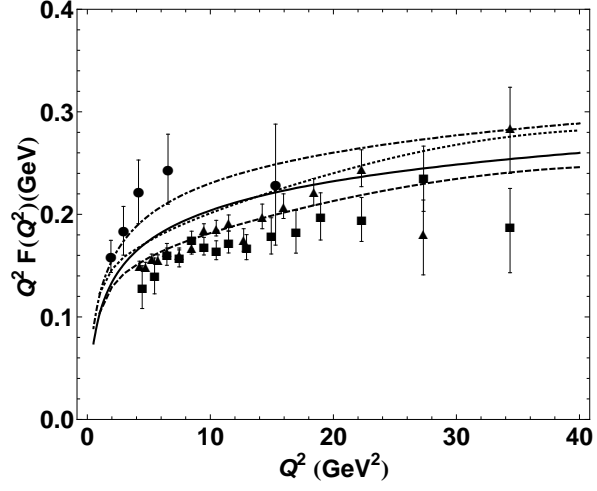
- [1] S. Catani, M. Ciafaloni and F. Hautmann, Phys. Lett. B **242**, 97 (1990); Nucl. Phys. **B366**, 135 (1991).
- [2] J.C. Collins and R.K. Ellis, Nucl. Phys. **B360**, 3 (1991).
- [3] E.M. Levin, M.G. Ryskin, Yu.M. Shabelskii, and A.G. Shuvaev, Sov. J. Nucl. Phys. **53**, 657 (1991).
- [4] J. Botts and G. Sterman, Nucl. Phys. **B325**, 62 (1989).
- [5] H.-n. Li and G. Sterman, Nucl. Phys. **B381**, 129 (1992).
- [6] T. Huang and Q.X. Shen, Z. Phys. C **50**, 139 (1991); J.P. Ralston and B. Pire, Phys. Rev. Lett. **65**, 2343 (1990).
- [7] S. Nandi and H.-n. Li, Phys. Rev. D **76**, 034008 (2007).
- [8] H.-n. Li, Y.-L. Shen, Y.-M. Wang, and H. Zou, Phys. Rev. D **83**, 054029 (2011).
- [9] H.-n. Li, Y.-L. Shen, and Y.-M. Wang, Phys. Rev. D **85**, 074004 (2012).
- [10] Y.C. Chen and H.-n. Li, Phys. Rev. D **84**, 034018 (2011).
- [11] Y.-Y. Charng and H.-n. Li, Phys. Rev. D **72**, 014003 (2005).
- [12] Y.C. Chen and H.-n. Li, Phys. Lett. B **712**, 63 (2012).
- [13] J.C. Collins, Acta. Phys. Polon. B **34**, 3103 (2003).

- [14] J.C. Collins and D.E. Soper, Nucl. Phys. **B193**, 381 (1981); J.C. Collins, Adv. Ser. Direct. High Energy Phys. 5, 573 (1989).
- [15] H.-n. Li, Y.-L. Shen and Y.-M. Wang, JHEP **1302**, 008 (2013).
- [16] J.L. Lim and H.-n. Li, Eur. Phys. J. C **10**, 319 (1999).
- [17] H.-n. Li, Phys. Lett. B **454**, 328 (1999).
- [18] E. Laenen, G. Sterman, and W. Vogelsang, Phys. Rev. Lett. **84**, 4296 (2000); Phys. Rev. D **63**, 114018 (2001).
- [19] G. Bozzi, B. Fuks, and M. Klasen, Nucl. Phys. **B794**, 46 (2008).
- [20] G. Sterman, Phys. Lett. B **179**, 281 (1986); Nucl. Phys. **B281**, 310 (1987).
- [21] S. Catani and L. Trentadue, Nucl. Phys. **B327**, 323 (1989); Nucl. Phys. **B353**, 183 (1991).
- [22] G.P. Korchemsky and G. Marchesini, Nucl. Phys. **B406**, 225 (1993); Phys. Lett. B **313**, 433 (1993).
- [23] J.C. Collins, D.E. Soper, and G. Sterman, Nucl. Phys. **B250**, 199 (1985).
- [24] H.-n. Li, arXiv:1308.0413 [hep-ph].
- [25] W. Lucha and D. Melikhov, J. Phys. G **39**, 045003 (2012); I. Balakireva, W. Lucha, and D. Melikhov, Phys. Rev. D **85**, 036006 (2012); D. Melikhov and B. Stech, Phys. Rev. D **85**, 051901 (2012); Phys. Lett. B **718**, 488 (2012).
- [26] H.-n. Li and S. Mishima, Phys. Rev. D **80**, 074024 (2009).
- [27] M. Beneke and T. Feldmann, Nucl. Phys. B **592**, 3 (2001).
- [28] I.O. Cherednikov and N.G. Stefanis, Nucl. Phys. **B802**, 146 (2008).
- [29] T. Kurimoto, H.-n. Li, and A.I. Sanda, Phys. Rev. D **65**, 014007 (2002).
- [30] G. Bell, T. Feldmann, Y.-M. Wang and M.W. Y. Yip, arXiv:1308.6114 [hep-ph].
- [31] P. Kroll, Eur. Phys. J. C **71**, 1623 (2011).
- [32] R. Jakob and P. Kroll, Phys. Lett. B **315**, 463 (1993) [Erratum-ibid. B **319**, 545 (1993)].
- [33] C.-D. Lü, W. Wang and Y.-M. Wang, Phys. Rev. D **75**, 094020 (2007).
- [34] A.V. Efremov and A.V. Radyushkin, Phys. Lett. B **94**, 245 (1980).
- [35] G.P. Lepage and S.J. Brodsky, Phys. Rev. D **22**, 2157 (1980).
- [36] A.V. Radyushkin, Phys. Rev. D **80**, 094009 (2009).
- [37] M.V. Polyakov, JETP Lett. **90**, 228 (2009).
- [38] T. Huang, T. Zhong, and X.G. Wu, Phys. Rev. D **88**, 034013 (2013); T. Huang, X.G. Wu, and T. Zhong, Chin. Phys. Lett. **30**, 041201 (2013).
- [39] S.S. Agaev, V.M. Braun, N. Offen and F.A. Porkert, Phys. Rev. D **83**, 054020 (2011); Phys. Rev. D **86**, 077504 (2012).
- [40] I.C. Cloët, L. Chang, C.D. Roberts, S.M. Schmidt and P.C. Tandy, Phys. Rev. Lett. **111**, 092001 (2013); L. Chang, I.C. Cloët, J.J. Cobos-Martinez, C.D. Roberts, S.M. Schmidt and P.C. Tandy, Phys. Rev. Lett. **110**, 132001 (2013).

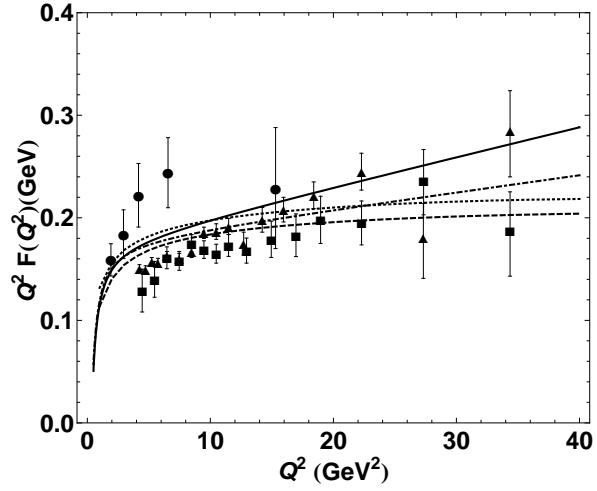
- [41] I.L. Solovtsov and D.V. Shirkov, Theor. Math. Phys. **120**, 1220 (1999) [Teor. Mat. Fiz. **120**, 482 (1999)].
- [42] A. Khodjamirian, T.Mannel, N.Offen and Y.-M.Wang, Phys. Rev. D **83**, 094031 (2011).
- [43] F.del Aguila and M.K. Chase, Nucl. Phys. B **193**, 517 (1981).
- [44] E. Braaten, Phys. Rev. D **28**, 524 (1983).
- [45] E.P. Kadantseva, S.V. Mikhailov and A.V. Radyushkin, Yad. Fiz. **44**, 507 (1986) [Sov. J. Nucl. Phys. **44**, 326 (1986)].
- [46] M. Nagashima and H.-n. Li, Phys. Rev. D **67**, 034001 (2003).
- [47] H.-n. Li and S. Mishima, Phys. Lett. B **674**, 182 (2009).
- [48] V.L. Chernyak and A.R. Zhitnitsky, Nucl. Phys. B **201**, 492 (1982) [Erratum-ibid. B **214**, 547 (1983)].
- [49] A.P. Bakulev and S.V. Mikhailov, Phys. Lett. B **436**, 351 (1998).
- [50] J. Gronberg *et al.* [CLEO Collaboration], Phys. Rev. D **57**, 33 (1998).
- [51] B. Aubert *et al.* [BaBar Collaboration], Phys. Rev. D **80**, 052002 (2009).
- [52] S.Uehara *et al.* [Belle Collaboration], Phys. Rev. D **86**, 092007 (2012).



(a)

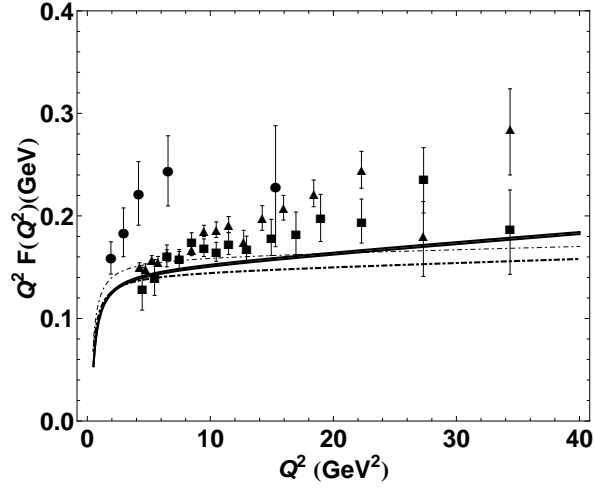


(b)

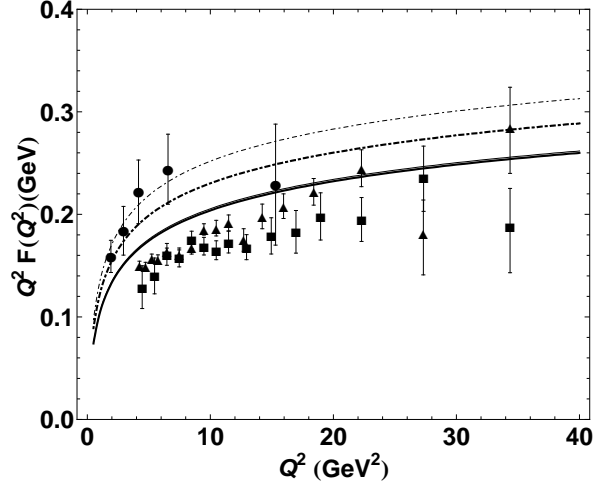


(c)

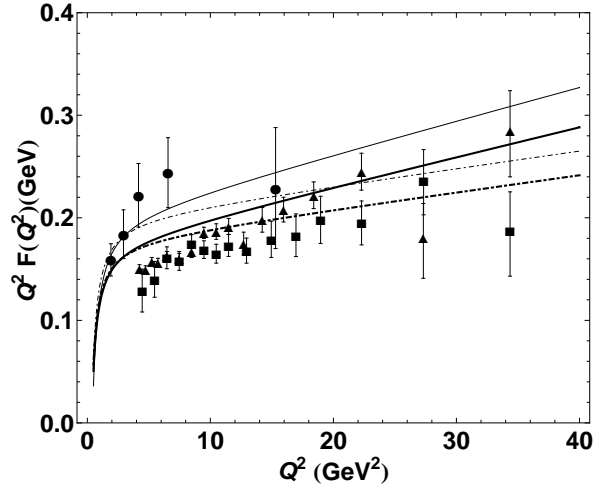
Figure 5: Pion transition form factor calculated from (a) the asymptotic model, (b) the flat model, and (c) the non-asymptotic model. The dashed and dotted (dot-dashed and solid) curves indicate the LO and NLO predictions from the conventional resummations (joint resummation). The experimental data are from CLEO [50] (dots), BaBar [51] (triangles), and Belle [52] (squares).



(a)



(b)



(c)

Figure 6: Hard scale induced uncertainties of the pion transition form factor for (a) the asymptotic model, (b) the flat model, and (c) the non-asymptotic model. The experimental data are from CLEO [50] (dots), BaBar [51] (triangles), and Belle [52] (squares). The (thin) dot-dashed and solid curves correspond to the LO and NLO predictions, respectively, under the joint resummation with $t = \max(\sqrt{x}Q, 1/b)$ ($t = \max(2\sqrt{x}Q, 1/b)$).